Available online at www.sciencedirect.com
SCIENCE DIRECT®
Archives of Biochemistry and Biophysics 433 (2005) 240–254
ABB
www.elsevier.com/locate/yabbi

Minireview

Bacterial defenses against oxidants: mechanistic features of cysteine-based peroxidases and their flavoprotein reductases☆

Leslie B. Poole*

Department of Biochemistry, Wake Forest University School of Medicine, Medical Center Blvd., BGTC, Winston-Salem, NC 27157, United States

Received 6 August 2004, and in revised form 8 September 2004
Available online 13 October 2004

Abstract

Antioxidant defenses include a group of ubiquitous, non-heme peroxidases, designated the peroxiredoxins, which rely on an activated cysteine residue at their active site to catalyze the reduction of hydrogen peroxide, organic hydroperoxides, and peroxynitrite. In the typical 2-Cys peroxiredoxins, a second cysteinyl residue, termed the resolving cysteine, is also involved in intersubunit disulfide bond formation during the course of catalysis by these enzymes. Many bacteria also express a flavoprotein, AhpF, which acts as a dedicated disulfide reductase to recycle the bacterial peroxiredoxin, AhpC, during catalysis. Mechanistic and structural studies of these bacterial proteins have shed light on the linkage between redox state, oligomeric state, and peroxidase activity for the peroxiredoxins, and on the conformational changes accompanying catalysis by both proteins. In addition, these studies have highlighted the dual roles that the oxidized cysteinyl species, cysteine sulfenic acid, can play in eukaryotic peroxiredoxins, acting as a catalytic intermediate in the peroxidase activity, and as a redox sensor in regulating hydrogen peroxide-mediated cell signaling.

Keywords: AhpF; AhpC; Peroxidase; Peroxiredoxin; Cysteine sulfenic acid; Disulfide reductase; Thioredoxin reductase; Redox-active disulfides; Flavoenzymes; Oxidoreductases

Bacterial defenses against peroxide-mediated oxidative damage include a family of non-heme, non-selenium proteins, distinct from catalases and glutathione peroxidases, which catalyze the reduction, and resulting detoxification, of organic hydroperoxides, hydrogen peroxide, and peroxynitrite [1,2]. Mechanistic studies have clarified the roles of reactive cysteinyl residues in the peroxidatic process and have highlighted the cascade of dithiol–disulfide interchange reactions that take place in support of this process. As the prototype peroxidase system, the studies described herein have focused on the alkyl hydroperoxide reductase proteins from *Salmonella typhimurium*, AhpC,[1] and AhpF [2,3], originally identified by Ames and co-workers [1] as part of the peroxide-responsive global regulon of the OxyR transcription factor. While the work reviewed here focuses on

☆ This work was supported in part by NIH RO1 GM50389 and an Established Investigatorship from the American Heart Association.
* Fax: +1 336 777 3242.
E-mail address: lbpoole@wfubmc.edu.

[1] *Abbreviations used:* AhpC, peroxidase component of the bacterial alkyl hydroperoxide reductase system, formerly known as C-22; AhpF, flavin-containing disulfide reductase component of the bacterial alkyl hydroperoxide reductase system, formerly known as F-52a; Cys-SOH, cysteine sulfenic acid; Prx, peroxiredoxin; TrxR, thioredoxin reductase; Trx, thioredoxin; F[1–202], truncated AhpF including residues 1–202; F[208–521], truncated AhpF lacking residues 2–20; NTD, N-terminal domain of AhpF; Nt-TrxR, chimeric protein expressed with residues 1–207 of AhpF followed by TrxR starting at residue 2; Cys165′, cysteinyl residue at position 165 on the partner subunit of the homodimer of AhpC; NBD chloride, 7-chloro-4-nitrobenzo-2-oxa-1,3-diazole; DTNB, 5,5′-dithiobis(2-nitrobenzoic acid); TNB, 5-thio-2-nitrobenzoic acid; NTSB, 2-nitro-5-thiosulfobenzoate; EH_2, two-electron reduced enzyme; EH_4, four-electron reduced enzyme; EH_6, six-electron reduced enzyme; pK_a, log of the acid dissociation constant; PDB, protein data bank.

0003-9861/$ - see front matter © 2004 Elsevier Inc. All rights reserved.
doi:10.1016/j.abb.2004.09.006

the *S. typhimurium* system, the results described are applicable to other bacterial systems, as well, and in the case of AhpC, to homologues present in a wide range of organisms. Thus, as our knowledge of these systems has expanded, it has become clear that AhpC, the peroxide-reducing protein of the system, is a representative of a very large and ubiquitous family of cysteine-based peroxidases, now designated as "peroxiredoxins" (Prxs). AhpF, on the other hand, is a flavoprotein expressed only by eubacteria and appears to act as a dedicated "AhpC reductase" in those bacteria which encode it (Fig. 1) [3–5]. In many AhpF-deficient organisms, the NAD(P)H-dependent recycling of AhpC or other Prxs is mediated by at least two proteins, either the thioredoxin reductase (TrxR) and thioredoxin (Trx) system, or related reductase systems specific to a particular organism or group of organisms. The following represents a discussion of mechanistic, structural, and biophysical studies of the cysteine-based peroxidases and their reductase systems from a number of bacteria, and the broader implications these studies have had on the biological roles these systems play in both prokaryotic and eukaryotic organisms.

Involvement of Cys residues in the mechanisms of both AhpC and AhpF

The peroxidase reaction catalyzed by AhpC does not involve bound heme or other metal or non-metal cofactors. Based on this observation and the precedent for peroxide reduction by a catalytic Cys residue in the streptococcal flavoprotein NADH peroxidase [6], our focus turned to the two Cys residues per subunit of AhpC, Cys46 and Cys165, as putative catalytic players in the peroxidatic mechanism (Fig. 1). In addition, the C-terminal most ~320 residues of AhpF are homologous with TrxR (35% identity) and contain the CXXCD motif required in TrxR for the dithiol–disulfide interchange reaction with Trx (corresponding to Cys345 and Cys348 in AhpF). Furthermore, AhpF possesses an additional ~200 residues at the N-terminus not present in TrxR, and the existence of another CXXC in this domain (Cys129 and Cys132) suggested an additional catalytic disulfide redox center. Thus, both CXXC motifs were hypothesized to be involved in the reduction of the putative AhpC disulfide bond for reactivation [7,8].

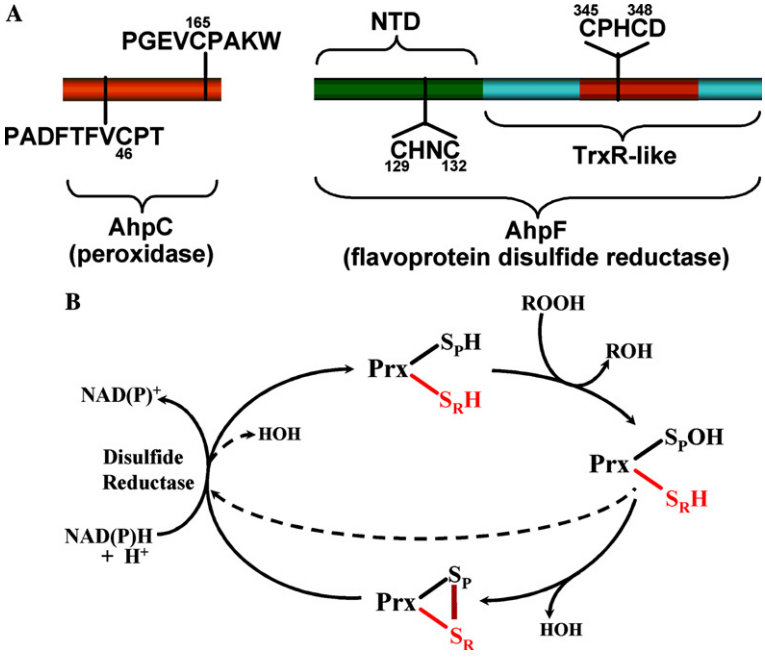

Fig. 1. Sequence arrangements of AhpC and AhpF (A) and the peroxidase catalytic cycle (B). In (A), catalytic Cys residues are shown, along with some surrounding sequence, for each alkyl hydroperoxide reductase system protein, AhpC and AhpF. The domain structure of AhpF is also depicted, with green representing the N-terminal domain (NTD), and the thioredoxin reductase (TrxR)-like C-terminal region of AhpF represented by the non-contiguous portions of the FAD-binding domain (blue) and by the NADH-binding domain (red). In (B), the peroxidatic Cys of the peroxiredoxin (Prx; e.g., AhpC) is depicted as a thiol (S_PH) or sulfenic acid (S_POH), or in a disulfide with the resolving Cys (S_RH). Colors distinguish the Cys residues from different subunits of the dimer in the typical 2-Cys Prxs, and the striped bar represents the intersubunit disulfide bond (intrasubunit in the case of the atypical 2-Cys Prxs). The disulfide reductase system varies with the organism, often being a Trx or Grx homologue and/or flavoenzyme (e.g., AhpF or TrxR), and utilizing at least one, and usually more, CXXC-containing proteins or domains. The pathway indicated by the dashed line can be taken by 1-Cys (no resolving Cys) or 2-Cys Prxs bypassing disulfide bond formation.

Electrophoretic and chemical analyses (using the thiol and disulfide detection reagents DTNB and NTSB, respectively) of oxidized forms of both AhpF and AhpC indicated the presence of two and one disulfide bond per subunit in the native enzymes, respectively [8]. Moreover, in AhpC, but not in AhpF, the disulfide bonds (two per homodimer) are intersubunit disulfides, covalently linking two subunits together; tryptic digests confirmed the linkage of Cys46 to Cys165′ (with the prime denoting that Cys165 of the pair resides in the partner subunit of the dimer) [8,9]. Upon anaerobic reduction by excess NADH, both disulfide centers of AhpF are reduced to thiols, yielding four nascent thiol groups. Stoichiometric reduction of AhpC by NADH (in the presence of a catalytic amount of AhpF) generated two free, accessible thiol groups in AhpC which were stoichiometrically reoxidized by ethyl hydroperoxide, supporting a catalytic role for these Cys residues in peroxide reduction by this protein. Thus, four Cys residues in AhpF (residues 129, 132, 345, and 348) and two Cys residues in AhpC (residues 46 and 165) are located within redox-active disulfide centers (Fig. 1A). Two remaining Cys residues in AhpF, Cys476 and Cys489, were shown to exist as free thiol groups in the native, oxidized protein, and through mutagenesis, were found to play no role in catalysis [8].

Multiple lines of evidence that the Cys thiol groups generated by reduction in the two proteins were, in fact, catalytic residues was obtained using alkylation by reagents such as *N*-ethylmaleimide (NEM), mutagenesis of Cys residues, and truncation by limited proteolysis. Thiol reagents reacted readily with the reduced (but not oxidized) forms of both proteins and completely inhibited peroxidase activity [10]. In AhpF, not only AhpC-dependent peroxidase activity, but also a less specific disulfide reductase activity (monitored by reduction of DTNB) was inhibited by alkylation or mutagenesis of either pair of Cys residues (Cys129-Cys132, or Cys345-Cys348) [10,11]. Limited tryptic digestion which removed the N-terminal domain of AhpF (as well as Cys129-Cys132) also eliminated these activities [8]. On the other hand, AhpF exhibits two other NADH-dependent activities, reduction of molecular oxygen (oxidase activity) and reduction of a higher redox potential NAD^+ analogue, 3-acetylpyridine adenine dinucleotide (transhydrogenase activity), which were unaffected by thiol reagents, Cys mutagenesis or proteolysis [8,10,11]. All these results were consistent with the presence of catalytic Cys residues in each protein of the bacterial peroxidase system.

Functional properties of AhpF: "modular" construction and large domain movements during catalysis

Sequence comparisons to TrxR (and Trx, see below) and functional studies indicate that AhpF plays the role in the peroxidase system of a pyridine nucleotide-dependent disulfide reductase, recycling AhpC for turnover with peroxide (Fig. 1). Like TrxR, electron transfer is mediated first by the transfer of a hydride from NADH or NADPH to the flavin, then progressive dithiol–disulfide interchange reactions among the redox-active disulfide centers in the flavoprotein and in the electron-accepting protein (e.g., Trx or AhpC). Much about these redox reactions can be inferred from spectral monitoring of the changes in the flavin redox state during static titrations or rapid reaction kinetic studies. Titrations with the chemical reductant dithionite show that the redox-active disulfide in the N-terminal domain (Cys129-Cys132) of AhpF is in functional communication with the TrxR-like disulfide center in the C-terminal portion (Cys345-Cys348) and with FAD (Fig. 2). Six electrons are required (two electrons each for the two disulfide centers, and another pair for the FAD) to fully reduce *S. typhimurium* AhpF [8] and homologues from three other species (*Streptococcus mutans*, *Amphibacillus*

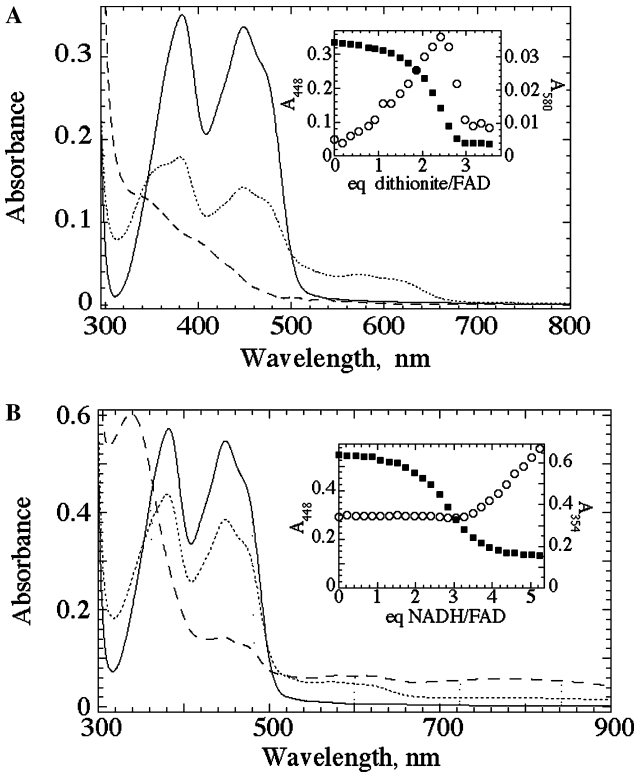

Fig. 2. Anaerobic dithionite (A) and NADH (B) titrations of Nox-1, the AhpF homologue from *Streptococcus mutans*. Spectra shown in (A) were obtained after the addition of 0 (solid line), 2.42 (dotted line), and 3.0 (dashed line) eq dithionite/FAD. The inset shows absorbance changes at 448 nm (closed squares) and 580 nm (open circles) during the course of the titration. Spectra shown in (B) were obtained after the addition of 0 (solid line), 2.84 (dotted line), and 4.81 (dashed line) eq NADH/FAD. The inset shows absorbance changes at 448 nm (closed squares) and 354 nm (open circles) during the course of the titration. Reprinted with permission from the *European Journal of Biochemistry* [3].

xylanus, and *Thermus aquaticus* [12–14]; see [3] for a review on these proteins). Two significant differences are observed between the spectral patterns obtained during reduction by dithionite and those using the physiological reductant, NADH. During dithionite (but less so NADH) titrations, a blue, neutral semiquinone form of the flavin is produced and stabilized in high amounts (Fig. 2A and [8]). This species has been shown to be generated, and disappear upon addition of oxidant, at such slow rates that it is clearly not a catalytically competent

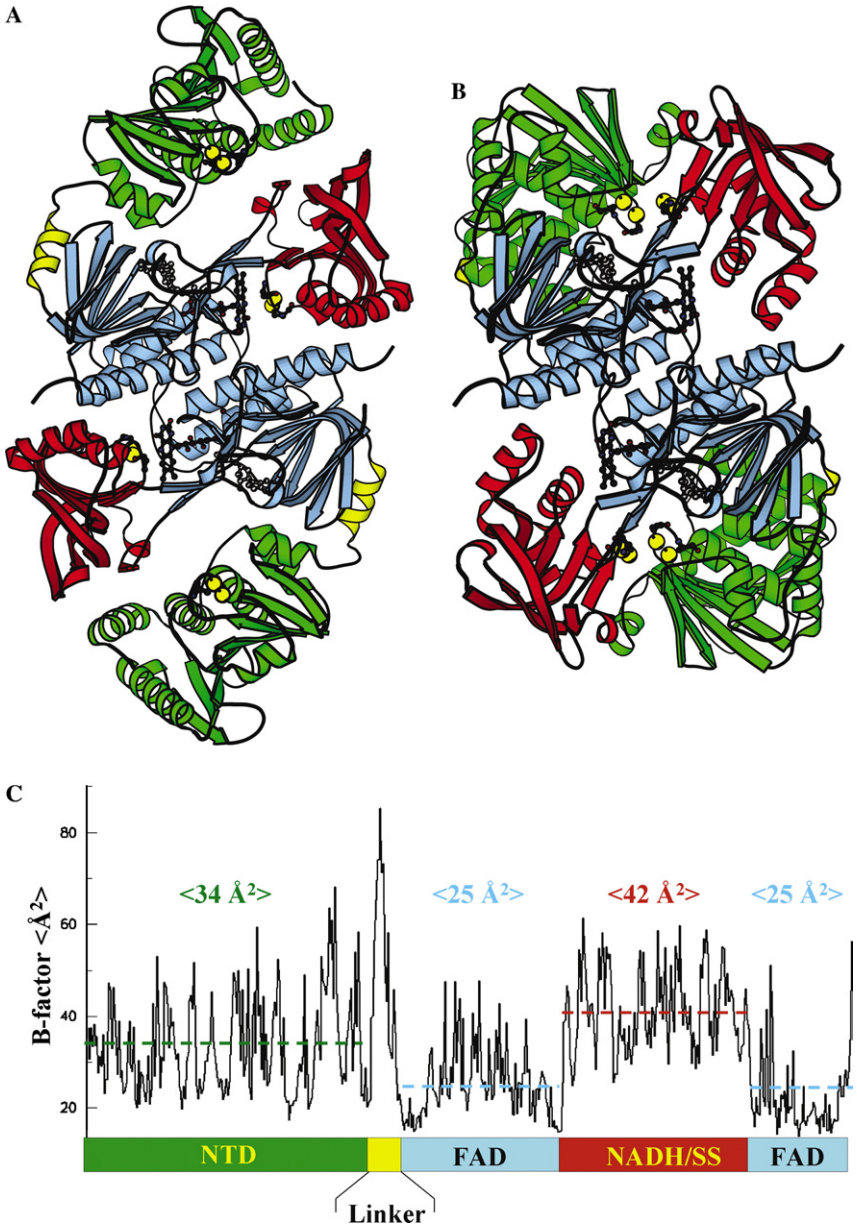

Fig. 3. Crystal structure (A), model of rotated domains (B), and *B*-factor plot (C) of AhpF. In (A), the AhpF dimer (pdb code 1hyu, 2.0 Å resolution [16]) is shown, colored by domains. The NTD (green), shown with its redox-active dithiol (Cys129,Cys132), is connected by the flexible linker (yellow) to the FAD domain (blue) and the NADH/SS domain (red), depicted with its redox-active disulfide (Cys345,Cys348). The bound flavin cofactor in the FAD domain is also shown. In (B), the hypothetical alternate conformation of AhpF that would allow for NTD reduction is depicted. Domains are colored as in (A), and the FAD domains are in the same orientations, to allow easy comparison. There are no steric clashes that would prevent the large-scale motions or final conformation proposed with the exception of a few surface sidechains that would require minor adjustments. The two redox-active disulfide centers are adjacent, and the NADH-binding site is now near the isoalloxazine ring. In order to achieve this conformation, a minimal change involves unraveling the first turn of the helix of the flexible linker (yellow). Such an unraveling of the linker helix is supported by limited proteolysis experiments [8]. Panel (C) illustrates the *B*-factors of the main chain atoms of AhpF plotted versus location in the primary structure, with coloring of domains similar to those in (A) and (B). Note the high degree of disorder of the linker and the different average *B*-factor values for each domain, strikingly illustrating the similarity in *B*-factors for the non-contiguous segments of the FAD domain. These average *B*-factor values support the suggestion that the three domains have different mobilities and can move independently from one another. Panels (A) and (B) are reprinted with permission from *Biochemistry* [16]. Copyright 2001 American Chemical Society. Panel (C) was kindly provided by Zachary A. Wood.

species for NADH-dependent turnover with AhpC. During NADH (but not dithionite) titrations of *S. mutans* Nox-1 and *S. typhimurium* AhpF, an additional prominent absorbance band is observed, extending beyond 900 nm, which arises from a charge-transfer interaction between $FADH_2$ and the bound NAD^+ (Fig. 2B and [8]). This species may represent a true catalytic intermediate given its rapid generation and AhpC-dependent oxidation ([15] and unpublished results from Li Calzi and Poole). Specificity for the pyridine nucleotide as assessed by both static titrations and kinetic assays (with DTNB as substrate) indicates that NADH is strongly favored over NADPH as a reductant [8,10]. AhpF homologues from gram positive organisms generally exhibit an even higher specificity for NADH [3].

The modular construction of AhpF as a TrxR-like flavoprotein disulfide reductase linked with a Trx-like CXXC-containing domain for electron shuttling to AhpC was implied by sequence comparisons (Fig. 1A) and modeling, then confirmed by X-ray crystallography and functional studies of the truncated proteins (Fig. 3) [16,17]. The N-terminal domain (NTD)-containing fragment, F[1–202], was generated (through protein engineering methods) based on the location of a tryptic-sensitive site on the C-terminal side of Arg202. The other fragment, F[208–521], encompassed the TrxR-like portion of AhpF, as supported by studies of a flavin-containing C-terminal tryptic fragment generated from limited proteolysis of AhpF [8]. The hypothesized sequence of electron transfers, from pyridine nucleotide to the flavin, then to the Cys345-Cys348 and subsequent Cys129-Cys132 centers of AhpF, followed by transfer to AhpC (Cys46-Cys165′), was firmly established through these studies. In brief, enzymatic assays, reductive titrations, and circular dichroism studies of the fragments indicated that each folds properly and retains many functional properties. Electron transfer between the two fragments was, however, relatively slow ($4 \times 10^4\ M^{-1}\ s^{-1}$ at 25 °C) and non-saturable with increasing F[1–202] up to 100 μM [17]; these protein "modules" are therefore much more efficient in interacting for electron transfer when attached to one another as in the native protein (k_{cat} for AhpF reacting with NADH and AhpC is $240\ s^{-1}$, and k_{cat}/K_m for AhpC is $\sim 1 \times 10^7\ M^{-1}\ s^{-1}$ at 25 °C) [12]. Interestingly, TrxR substituted for F[208–521] was essentially as efficient a reductant of F[1–202] as was F[208–521] (within about 2-fold). (TrxR is, in this sense, more "promiscuous" than AhpF; neither F[208–521] nor full-length AhpF can reduce Trx.) Interestingly, a chimeric construct, the NTD attached to the N-terminus of *Escherichia coli* TrxR (Nt-TrxR), demonstrated full competence of TrxR as a replacement for F[208–521] in a full-length AhpF-like protein [18]. Moreover, the CXXC center of the F[1–202] fragment was shown to have the same reduction potential (−270 mV) as Trx; this pre-reduced

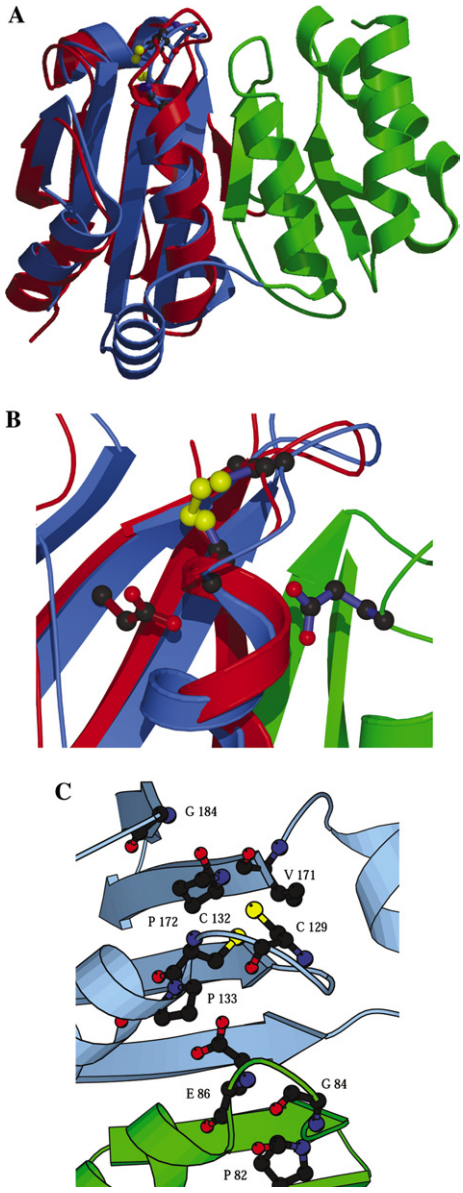

Fig. 4. Structure of the AhpF NTD and comparisons with *E. coli* thioredoxin (Trx). (A) and (B) ribbon representations of the AhpF NTD (residues 1–195) with separate colors for the two Trx-like folds (green for the N-terminal half, blue for the C-terminal half), and an overlay of the C-terminal half of the NTD with *E. coli* Trx (red) based on Cα atoms (r.m.s.d. is 2.5 Å for 85 equivalent Cα atoms). As illustrated most clearly in the close-up view of (B), the redox-active cysteines/cystine for both enzymes are shown in ball-and-stick representations, as are Glu86 (contributed by the first Trx fold to the active site lying predominantly in the second Trx fold) of the NTD (blue bonds) and Asp26 of *E. coli* Trx (red bonds). The carboxylates of both acids and all four of the sulfurs of the active sites lie in the same plane, with the carboxylates in the same relative orientations and distances with regard to the interchange thiol, albeit with their positions reflected through an approximate mirror containing the interchange thiol sulfur atom. (C) The arrangement of residues within the NTD active site, with Trx folds colored as in (A) and (B). All nine absolutely conserved residues among five NTD homologues are shown (for details, see Fig. 4A [16]). Cys132-Sγ is completely solvent inaccessible, while Cys129 is on the surface and exposed. Note that Pro82, Gly84, and Glu86 all derive from the first Trx fold. Panel (C) is reprinted with permission from *Biochemistry* [16]. Copyright 2001 American Chemical Society.

fragment could act independently of F[208–521] as an efficient electron donor to AhpC (unlike the F[208–521] itself) [17,18]. Thus, the NTD of AhpF, specifically through its Cys129-Cys132 disulfide center, was firmly established as the direct electron donor to the intersubunit disulfide bond of AhpC [8,11,17,18].

The NTD is itself a fascinating protein "module" for which an independently expressed homologous protein, named "protein disulfide oxidoreductase," exists in some thermophiles [16,17,19]. These proteins represent a new class of protein disulfide reductases composed of two tandem Trx folds (so intimately associated as to be considered a single domain), but with a functional disulfide redox center only in the second of the two folds. Interestingly, the residues around this active site include a carboxylate (Glu86 in AhpF) being contributed by the first Trx fold in a pseudo-mirrored position relative to, and functionally equivalent to, the carboxylic acid (Asp26) of *E. coli* Trx (Fig. 4) [16]. Furthermore, fortuitous reduction of the NTD redox center, Cys129-Cys132, in the synchrotron (Roberts and Karplus, unpublished observations) gave a detailed view of the thiol–thiolate hydrogen-bonding interaction (3.04 Å distance between sulfurs) at this active site [16].

Both the functional studies of the truncated proteins and the AhpF structure as determined by X-ray crystallography (at 2.0 Å resolution) imply large domain rotations during catalysis [16,17]. As illustrated in Figs. 1 and 3, the homodimeric protein consists of three interacting domains: the NTD (residues 1–196) containing the AhpC-interacting redox-active disulfide (Cys129-Cys132), the flavin-binding (FAD) domain (residues 210–327 and 450–521) attached to the NTD via a flexible linker (residues 197–209), and the NADH-binding and redox-active disulfide-containing (NADH/SS) domain (residues 328–449) (green, blue, and red, respectively, in Fig. 3). Whereas the FAD domain, comprised of two non-contiguous sequences, can be viewed as relatively immobile (average *B*-factor of 25 $Å^2$ for main chain atoms, Fig. 3C) and contributing to essentially all of the interactions stabilizing the antiparallel homodimer, the NADH/SS domain (average *B*-factor of 42 $Å^2$) likely swings through an approximate 67° arc in a fashion similar to the corresponding domain of TrxR [20]. This rotation alternately brings the nicotinamide ring of the pyridine nucleotide, or the Cys345-Cys348 disulfide center, into position over the isoalloxazine ring of the flavin for electron transfer (Fig. 5). Although only a single conformation of the NADH/SS domain with respect to the FAD domain has so far been observed for AhpF, wherein the Cys345-Cys348 redox center is proximal to the flavin

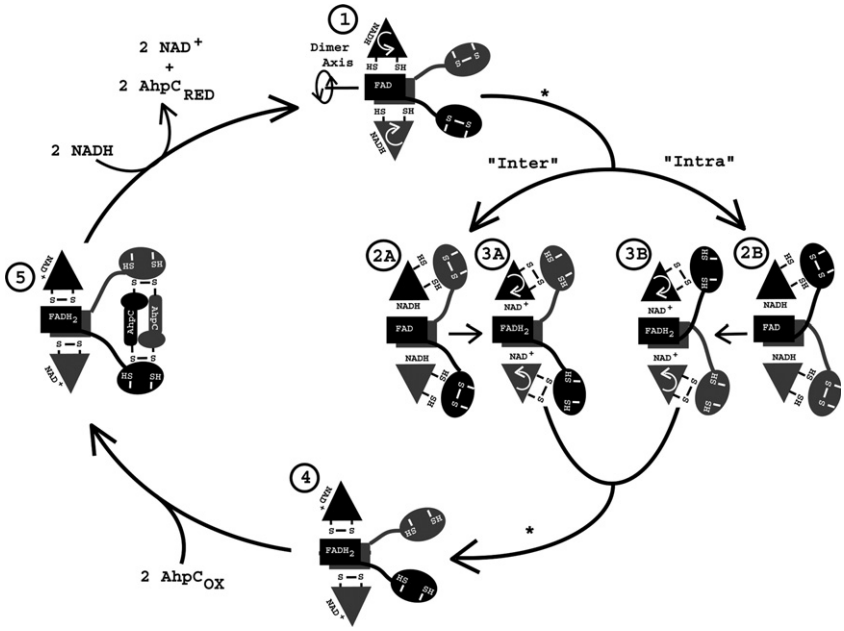

Fig. 5. Putative conformational changes taking place during the catalytic cycle of AhpF. The proposed catalytic cycle of dimeric AhpF is shown, oriented with the dimer axis of AhpF in the plane of the figure. Individual subunits are colored gray or black. The NADH domain (triangle) is shown with either NAD^+ or NADH bound, and its redox center (Cys345,Cys348) in either the oxidized (S-S) or reduced $(SH)_2$ form. White circular arrows denote domain rotations. The FAD domain (rectangle) has either oxidized (FAD) or reduced ($FADH_2$) flavin. The redox center (Cys129,Cys132) of the NTD (ovals) is depicted in either the oxidized (S-S) or reduced $(SH)_2$ form. Both theoretical pathways for electron transfer to achieve NTD reduction, intersubunit (via **2A** → **3A**) and intrasubunit (via **2B** → **3B**), are illustrated, although experimental and modeling approaches have confirmed that only the intrasubunit pathway is functional. Asterisks in the paths indicate conformational changes. AhpC is represented as $AhpC_{OX}$ (oxidized) or $AhpC_{RED}$ (reduced). For simplification, reactions and conformational changes in both subunits of the dimer or with AhpC are depicted as synchronous events. Reprinted with permission from *Biochemistry* [16]. Copyright 2001 American Chemical Society.

and the putative NAD-binding site is exposed, a model of the alternate conformation based on the "twisted" structure of a TrxR–Trx complex (pdb code 1f6m [16]) has been constructed (Fig. 3B). Furthermore, with one particular doubly mutated AhpF construct (C132, 345S), but not with the other three double mutant combinations, DTNB treatment (to induce disulfide bond formation) generates a covalent disulfide linkage between the two redox centers, locking the rotated NADH/SS domain, as well as the NTD, into a structure likely to closely resemble the "twisted" model [21]. This "locked" conformation exhibits considerably higher resistance to proteolytic cleavage and cannot be "unlocked" by addition of NADH (although the flavin is still reducible), consistent with a restricted conformation for this engineered protein and with the location of the "inter-center" disulfide bond (linking the two cysteinyl redox centers) remote from the flavin.

There must also be very large conformational changes to allow for the NTD to interact with the NADH/SS domain to receive the NADH-derived electrons (as depicted in the "twisted" model, Fig. 3B), then rotate away from this position for electron-transfer interactions with its protein substrate, AhpC. The crystal structure, wherein the NTD is "frozen" through crystal contacts into a conformation that may or may not be particularly relevant to its solution conformations, indicates *B*-factors and a lack of significant inter-domain interactions that are consistent with NTD mobility. The average *B*-factor for main chain atoms is higher than for the FAD domain, at 34 $Å^2$ (Fig. 3C) and the NTD is connected to that domain through a poorly ordered loop-helix linker depicted in yellow in Fig. 3 (average *B*-factors for residues 197–200 of the loop and for residues 201–203 of the helix are >70 and >50 $Å^2$, respectively). The intriguing result that the chimeric protein (Nt-TrxR) retains full activity as a Trx reductase [18] also implies that the NTD can rotate away from the NADH/SS (or NADPH/SS in TrxR) domain far enough to allow Trx to access the dithiol center in the pyridine nucleotide-binding domain with little or no restriction. An initial hypothesis that the electron-transfer pathway between the dithiol/disulfide centers in the NADH/SS and NTD domains was an intersubunit process was formulated, in the absence of high-resolution structure information, based on the putative antiparallel arrangement of subunits and the attachment of the NTD to the FAD domain at a position remote from the NADH/SS domain of its own subunit ([17] and Fig. 5, pathway with 2A and 3A). However, both the modeling studies described above [16] and experimental data [22] have confirmed intrasubunit electron transfer between these domains (Fig. 5, pathway with 2B and 3B) and ruled out a functional intersubunit transfer pathway. To show this, two heterodimeric AhpF species were created in which one of the two pathways was completely disrupted while the other was left partially intact in each construct [22]. Only the heterodimers containing one monomer of wild type AhpF and a monomer of mutated (and truncated) AhpF exhibited peroxidase activity with AhpC, indicating that electron transfer between domains of AhpF is an intrasubunit process.

Taking all of these putative domain rotations into account, a minimal mechanism for turnover of AhpF invoking two conformational changes (and two predominant conformations) per cycle has been proposed [3,17]. This proposal includes coordinated rotations by both the NADH/SS and NTD domains to alternate between interacting pairs of redox centers, and the cycling of AhpF (and other orthologous proteins) between their two electron-reduced and four electron-reduced redox states (EH_2 and EH_4 by standard flavin nomenclature) during rapid turnover (Fig. 5). (Priming by a single equivalent of NADH to generate EH_2 would be required to initiate the cycle depicted; Fig. 5 in [3].) Although our understanding of the motions and factors involved in coordination of these motions is far from complete, there is at least some experimental evidence suggesting that a fully reduced form of the *A. xylanus* AhpF homologue, EH_6, is not kinetically competent [15], consistent with this proposal.

Experiments have also been conducted to better understand the nature of the complex between AhpF and AhpC, transiently linked through an "inter-protein" disulfide bond, which must be generated during dithiol–disulfide interchange to transfer electrons. The purified proteins free in solution have not been observed to interact non-covalently except for the special case of the AhpF and AhpC homologues from the thermophilic bacterium, *T. aquaticus*, where the two proteins were difficult to separate [14]. This point is emphasized as some investigators have misconstrued the discussion of AhpF–AhpC complexes being formed during catalysis as indicating that they exist in solution as subunits of a heteromeric "holoenzyme" [23,24]. To learn more about the roles of particular Cys residues in AhpF and AhpC and to obtain stabilized mimics of putative catalytic intermediates, mutants of each protein lacking one active site Cys were combined, following oxidation of one of the two proteins by DTNB (to generate the disulfide-linked TNB conjugate), and analyzed for the rates and extents to which disulfide bond formation between the two proteins occurred ([25] and Ellis, Jönsson, and Poole, unpublished). In the direction of electron transfer which best simulates catalysis (AhpF reduced and AhpC oxidized), only one of the four mutants of AhpF, C132S, and only one of the two mutants of AhpC, C46S, generated a significant amount of higher molecular weight complex. This complex formed with a second-order rate constant of about $2 \times 10^6\ M^{-1}\ s^{-1}$ (comparable to the k_{cat}/K_m for AhpF turnover with AhpC of about $10^7\ M^{-1}\ s^{-1}$). As with the Cys129-Cys348 covalent link-

age in the DTNB-treated C132,345S AhpF mutant described above, the "engineered" disulfide bond between Cys129 of AhpF and Cys165 of AhpC is not reducible by NADH. In these cases, the putative domain movements required for electron transfer are likely to be restricted by the covalent attachment of the second protein (or domain). These results are analogous, also, to the stability of the TrxR–Trx complex between the C135S and C32S mutants, respectively, of those proteins [26]. We conclude from these studies that Cys129 is the nucleophile of the AhpF NTD that attacks the intersubunit disulfide bond of oxidized AhpC at Cys165 to initiate electron transfer between the two proteins, and that the engineered covalent complex between the proteins generated by the mutants as described above represents a reasonable mimic of the transiently formed intermediate during this transfer.

The Cys-based peroxidatic mechanism of AhpC involves a Cys sulfenic acid intermediate and optional disulfide bond formation

Given the lack of metal or prosthetic groups in AhpC and the enzymological and mutagenic data described above, the focus of investigations into its peroxidatic activity was on the Cys residues. Studies of AhpC single Cys mutants were invaluable in elucidating the mechanism of AhpC reaction with hydroperoxide substrates. The AhpC C165S variant, retaining the conserved Cys46 thiol, was fully active as a peroxidase when NADH and AhpF were present in excess amounts in the assay, while the C46S mutant (as well as C46,165S) was completely inactive under any conditions [9]. The Cys thiol (Cys46-SH) of the C165S mutant (but not Cys165-SH of C46S) was oxidized by one equivalent of H_2O_2 or cumene hydroperoxide, a process which was reversible by addition of a single equivalent of NADH (in the presence of a catalytic amount of AhpF).

Initial evidence that the oxidized Cys species formed in the first step of the peroxidase reaction is a sulfenic acid (Cys-SOH) was obtained through demonstration of its reactivity toward TNB and dimedone and its susceptibility to further oxidation (sometimes referred to as overoxidation) by peroxides and oxygen [9,27]. Most convincing, however, was the novel trapping method for Cys-SOH developed during the course of these studies [27]. Using NBD chloride as a labeling agent, the respective adducts of Cys46-SH and Cys46-SOH could be clearly distinguished by their visible absorbance properties ($\lambda_{max} = 420$ nm for Cys46-S-NBD and 347 nm for Cys-S(O)-NBD) and molecular mass by electrospray ionization mass spectrometry (20,765 versus 20,781 amu, respectively) (Fig. 6). This method has subsequently been used to demonstrate Cys-SOH formation in the C165S mutant of AhpC as a result of peroxynitrite reaction [28], as well as peroxide- or substrate-mediated Cys-SOH formation in a number of other proteins [29–34].

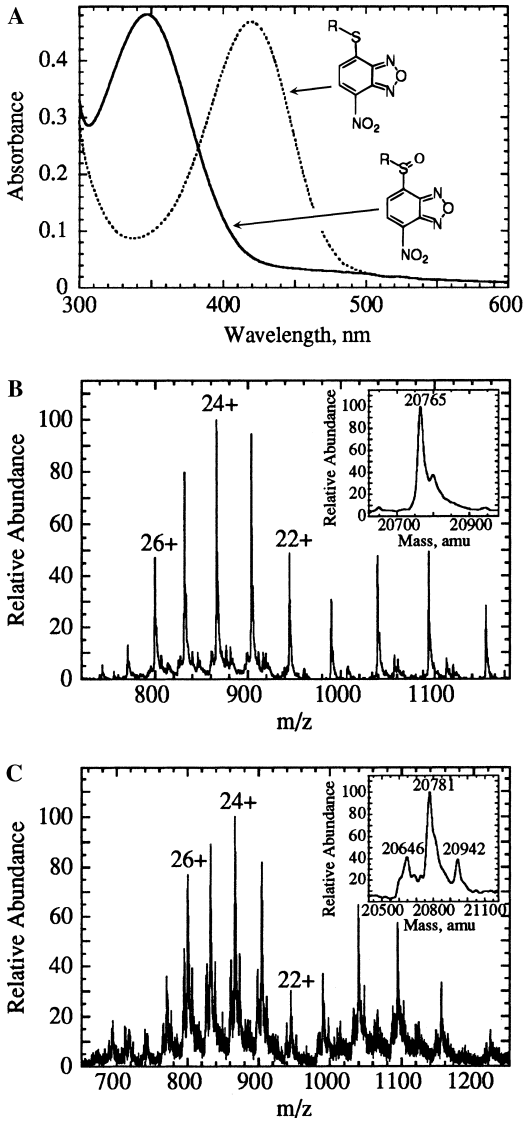

Fig. 6. NBD adducts of cysteine thiols and sulfenic acids in *S. typhimurium* AhpC. The reduced (R-SH) and oxidized (R-SOH) forms of the C165S mutant of AhpC give rise to distinctive spectra (A) with maxima at 420 nm (R-S-NBD, the thioether adduct, dotted line) and 347 nm (R-S(O)-NBD, the putative sulfoxide adduct, solid line), respectively. Unlike R-S(O)-NBD, R-S-NBD is also fluorescent. The identity of these adducts was confirmed by electrospray ionization mass spectrometry, yielding masses of 20765.2 (B) and 20781.5 atomic mass units (C) for R-S-NBD and R-S(O)-NBD, respectively. The plots are reprinted with permission from *Biochemistry* [27]. Copyright 1997 American Chemical Society.

While these were the first studies which directly established the intermediacy of Cys-SOH in the Prx peroxidatic mechanism, precedent for this enzyme-mediated chemistry had already been set by studies of an enterococcal flavin-containing peroxidase, NADH peroxidase, that contains only a single Cys residue per subunit and does not form disulfide bonds during catalysis [6,35].

This chemistry is also directly analogous to that used by glutathione peroxidases, although in those enzymes the selenocysteine is the active site residue attacking the –O–O– bond [36].

As reactivity of Cys thiol groups (in their protonated state) toward peroxides is insignificant in the absence of catalytic quantities of metals (particularly iron and copper) [37], lowering of the pK_a of the peroxidatic Cys residue in Prxs is likely essential for their function. While the exact pK_a of the peroxidatic Cys in AhpC or other Prxs is not currently known (estimates have included values lower than 5 [28], and a value of 4.6 for the related Cys of PrxVI [38]), it is likely lowered from an ''unperturbed'' value of approximately 8.5–9.5 [38,39] by some of the same forces that stabilize the sulfenate anion of the oxidized protein [40]. Electrostatic interaction with an absolutely conserved Arg residue in the active site (Arg119 in AhpC), and hydrogen bonding to a highly conserved Thr residue (Thr43 in AhpC, replaced in a few Prxs by Ser), are likely to be important contributors to enhanced stability of the thiolate (and presumably sulfenate) anion(s) (Fig. 7C) [41,42]. As is often the case for redox-active Cys residues [43], the active site thiol(ate) sits at the N-terminus of an α-helix, perhaps influenced by the dipole moment of this helix. Presence of a catalytic acid in the active site to protonate the RO^- leaving group as formed during the first catalytic step is also inferred by this mechanism, although such a residue has yet to be identified in the Prxs [42].

In the second step of the peroxidase mechanism, the nascent sulfenic acid in the active site of wild type AhpC, Cys46-SOH, is attacked by the Cys165 thiol(ate) of an adjacent subunit to form the intersubunit disulfide bond (Fig. 1B) [9]. In fact, resolution of the active site Cys-SOH through protein disulfide bond formation is characteristic of most, but not all, Prxs. Mechanistic distinctions among Prxs at this step have led to the delineation of three categories of Prxs. Based on the conservation, and involvement in catalysis, of either one or two Cys residues in the Prxs, this large family was originally divided into 1-Cys and 2-Cys sub-families [5]. The 2-Cys Prxs were then further divided into two classes designated as the ''typical'' (intersubunit disulfide bond-containing) and ''atypical'' (intrasubunit disulfide bond-containing) 2-Cys Prxs [42].

While disulfide bond formation prior to reaction with the reductant is common, it is by no means required for catalysis. This is demonstrated both by the existence of functional 1-Cys Prxs, and by the conversion of the typical 2-Cys Prx, AhpC, into a fully active 1-Cys Prx by mutagenesis of Cys165. The functional importance of the ''resolving'' Cys in the 2-Cys Prxs is highlighted by the enhanced susceptibility of C165S AhpC toward inactivation by its own substrate; the oxidized form of the wild type enzyme is highly resistant to peroxide-mediated inactivation due to disulfide bond formation between the two Cys residues, rather than persistence of the reactive Cys-SOH at the active site [9,44]. (This lack of sensitivity toward peroxide inactivation is a characteristic that distinguishes bacterial AhpC homologues from many eukaryotic Prxs, an issue of critical importance to their distinctive roles in these organisms, as described in the next section.) Evidence elaborated above also supports a role for Cys165 of AhpC as the point of attack by the nucleophilic Cys residue of AhpF, Cys129, to initiate electron transfer [25]. Still, AhpF is able to efficiently recycle the Cys46-SOH form of the C165S mutant of AhpC during catalysis, even though the flavoprotein has presumably evolved as a disulfide (rather than Cys-SOH) reductase for reactivating the wild type peroxidase.

Given these mechanistic considerations, as well as the limited conservation and variable location of the resolving Cys in the Prx family members, this residue must have arisen, and perhaps even disappeared again, at various times during the evolution of the Prxs. This conclusion is supported by recent sequence and structure analysis exploring the divergence of the Prxs from Trx-like ancestral proteins [45]. In these studies, four evolutionarily distinct groups of Prxs were identified based on conserved and presumably functional residues in proximity of the active site, with less emphasis on the presence and location of the resolving Cys.

Changes in conformational and oligomeric states of AhpC effected by redox cycling: structural evidence for a biological role for Prxs in regulation of hydrogen peroxide-mediated cell signaling in higher organisms

Since 1998, approximately a dozen crystal structures of Prxs have been solved and deposited in the Protein Data Bank. These structures show the 1-Cys and typical 2-Cys Prxs to be antiparallel homodimers, containing an extended β-sheet at their core, which may associate into toroid-shaped $(\alpha_2)_5$ decamers (Figs. 7A and B) [42]. As shown by the two decameric structures of *S. typhimurium* AhpC representing different redox states of the enzyme, considerable conformational rearrangements must take place during catalysis (Fig. 8C) [41,44]. Within the disulfide bond between Cys46 and Cys165 on an adjacent subunit of the oxidized enzyme, the two sulfur atoms are situated about 2 Å from one another (Fig. 8C, right); however, in the reduced-like C46S structure, the Cys residues are oriented in opposite directions (~13 Å between sulfur atoms) (Fig. 8C, left). The activated enzyme, ready for peroxide reduction, holds the sulfur of the peroxidatic Cys at the N-terminus of an α-helix in optimal position with respect to the conserved residues (including Thr43 and Pro39) in the preceding loop (the active site loop-helix), as well as the conserved Arg119 (Fig. 7C). Upon reaction, the Cys-SOH must become

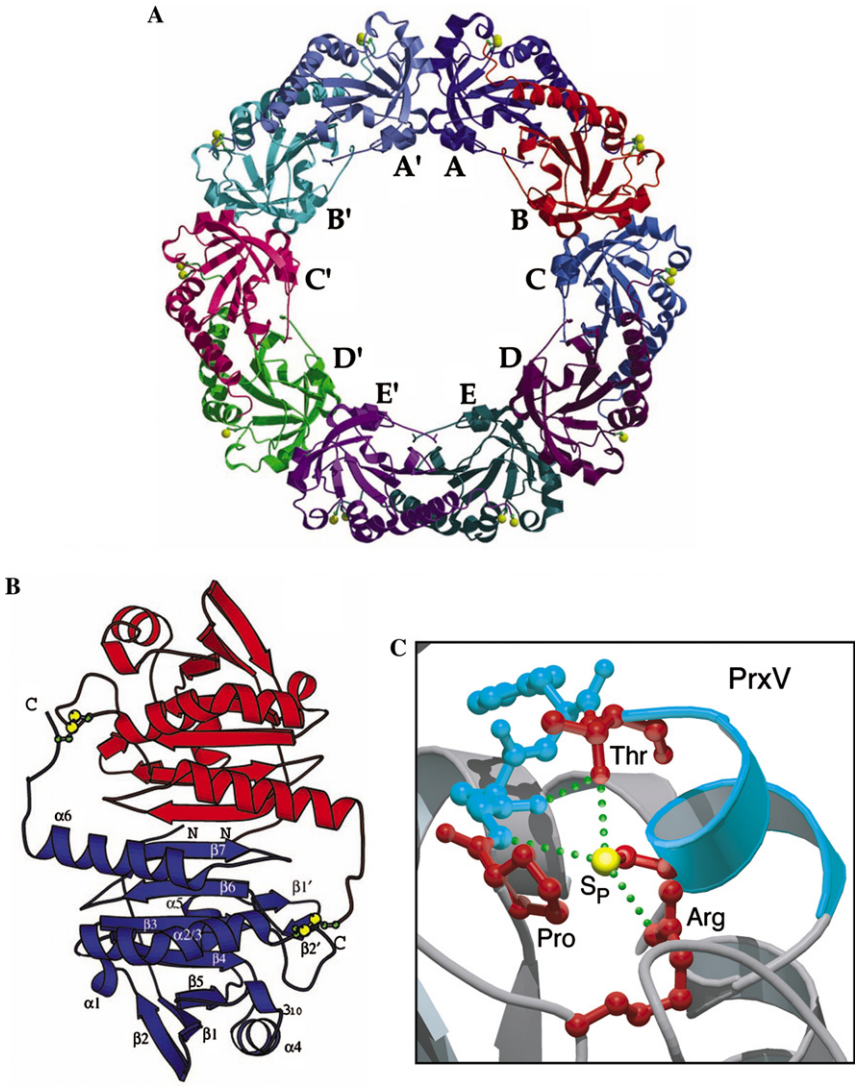

Fig. 7. The $(\alpha_2)_5$ decameric structure (A) of *S. typhimurium* AhpC and its component homodimer (B), and structural details of the conserved active site from the prototypic PrxV structure (C). In (A), the $(\alpha_2)_5$ decamer (from the X-ray crystal structure of oxidized AhpC solved at 2.5 Å resolution; pdb code 1kyg [41]) is shown with each chain depicted in a different color. The individual chains are are labelled A, B, C, D, and E, with primes denoting their crystallographic symmetry mates. Dimers are A–B, C–D, and E–E′. The crystallographic 2-fold axis bisects the homodimer (E–E′) and the interface between two dimers (A–B and A′–B′). Redox-active disulfides are depicted as ball-and-stick models, with sulfurs in yellow. Panel (B) depicts the AhpC α_2 dimer, with monomers in different colors and looking down the dimer axis. The intersubunit redox-active disulfides are depicted as in (A). The C-terminal arm containing the resolving Cys reaches across the interface and is rather flexible. Density for residues beyond the resolving Cys was missing in this structure. Panel (C) illustrates the conserved, reduced Prx active site (shown using the PrxV structure, pdb code 1hd2 [64]) and the conserved hydrogen-bonding network (dotted lines). The active site residues conserved in all Prxs (Pro, Thr, Cys, and Arg) are colored red, and the loop-helix region is colored blue. Panels (A) and (B) are reprinted with permission from *Biochemistry* [3], and panel (C) is reprinted with permission from *Trends in Biochemical Sciences* [42]. Copyrights 2000 American Chemical Society, and 2002 Elsevier Science Ltd.

exposed through local unfolding for disulfide bond formation, unraveling a turn of the helix. In addition, the C-terminal arm must unfold to bring the resolving Cys into proximity of the Cys-SOH; in the disulfide bond-containing forms of the typical 2-Cys Prxs for which structures are known (rat PrxI, 1qq2 [46]; and *S. typhimurium* AhpC, 1kyg [41]), the C-terminal arm is disordered beyond the resolving Cys, indicating a high degree of mobility for this locally unfolded segment (Figs. 8B and C, right sides).

Of these two disulfide bond-containing structures, the PrxI was dimeric, while the oxidized AhpC was decameric. The other two typical 2-Cys Prx structures known at the time, *Crithidia fasiculata* tryparedoxin peroxidase (1e2y [47]) and human PrxII (1qmv [48]), were both decameric and represented reduced and overoxidized (sulfinic acid) Prx forms, respectively [42]. To better understand the relationship between dimeric and decameric species of typical 2-Cys Prxs, analytical ultracentrifugation studies of *S. typhimurium* AhpC were

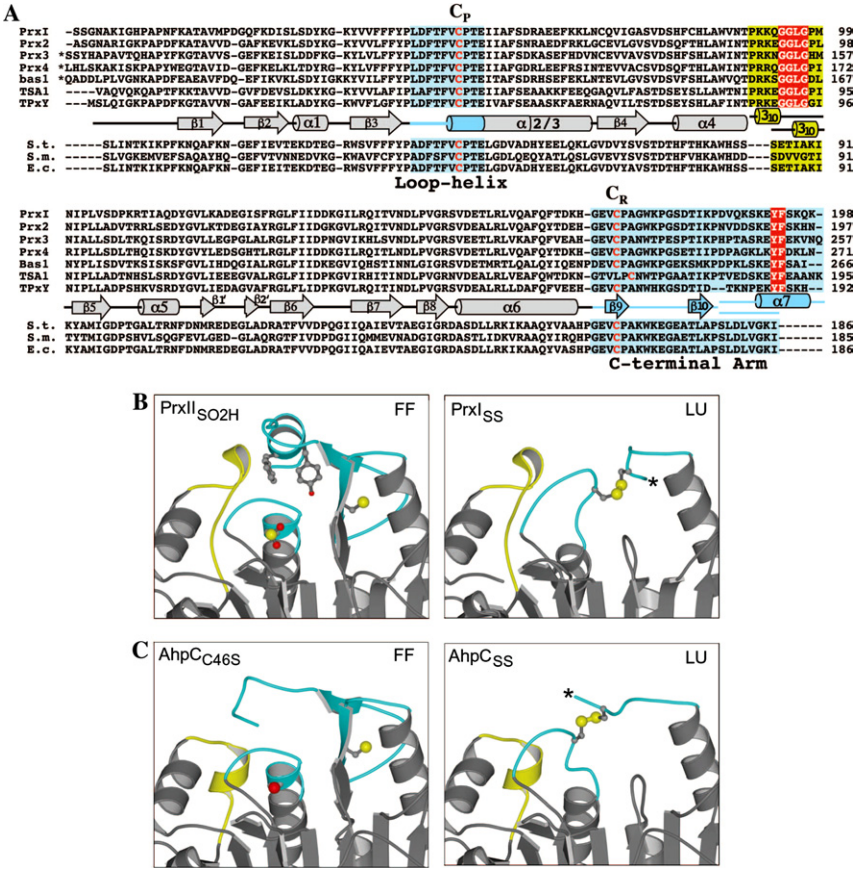

Fig. 8. Structural differences between robust and sensitive 2-Cys Prxs. (A) A structure-based sequence alignment of seven 2-Cys Prxs that have been documented to be sensitive (top group of sequences) versus three 2-Cys Prxs that have been documented to be robust (lower group of sequences). Secondary structure elements are depicted as helices (cylinders) or strands (arrows), with structural differences as disconnected elements (yellow or cyan). The shifted 3_{10} helix and loop (yellow) and regions which undergo conformational rearrangements during catalysis (cyan) are identified. The GLGG and YF motifs are highlighted in red, and the peroxidatic (C_P) and resolving (C_R) cysteines are depicted. Sensitive 2-Cys Prx sequences shown are human PrxI [53,65], PrxII [65,66], PrxIII [65,67], and PrxIV [65], yeast TSA1 [68], yeast TPxY [69] and plant BAS1 [70], and robust 2-Cys Prx sequences shown are AhpC from *Salmonella typhimurium* [71], from *Streptococcus mutans* [12], and from *Escherichia coli* [59]. (B) Ribbon diagrams of the peroxidatic active site region of sensitive 2-Cys Prx structures for the fully folded (FF) and the locally unfolded (LU) conformations. Elements are colored as in (A), with side chains for C_P, C_R, and the YF motif included. Panel (C) is similar to (B), but for a robust enzyme (AhpC). Structures shown are as follows: panel B (FF), SO_2H form of human PrxII (pdb code 1qmv [48]); panel B (LU), disulfide form of human PrxI (pdb entry 1qq2 [46]); panel C (FF), C46S form of *S. typhiumurium* AhpC (pdb code 1n8j [44]); and panel C (LU), the disulfide form of *S. typhiumurium* AhpC (pdb code 1kyg [41]). Asterisks marking the ends of the visible C-termini of the LU conformations indicate that many additional C-terminal residues are disordered. Although PrxII$_{SO2H}$ is an inactive enzyme, it is known to adopt the same conformation as active, reduced 2-Cys Prxs [48]. Comparison of the FF panels of (B) and (C) provides the most dramatic image of how the two sequence features common to sensitive enzymes result in a major difference in the burial of the C_p-containing helix. Reprinted with permission from *Science* [44]. Copyright 2003, American Association for the Advancement of Science.

performed. Using a variety of loading concentrations and both equilibrium and velocity experiments, the reduced enzyme was shown to be decameric at all concentrations tested, while the oxidized enzyme was a mixture of species at most concentrations, but purely dimeric at 2.5 μM and purely decameric at 480 μM (Fig. 9) [41]. Thus, the crystal structure of oxidized AhpC represents a metastable oligomerization intermediate favored by the high protein concentrations used for crystallization.

Incorporating these findings into a structurally detailed catalytic cycle linking oligomeric state with activity, Fig. 10 illustrates the stabilizing effects of the decameric structure on the active site loop-helix, with the dimer–dimer interface acting to buttress this flexible region. Upon local unfolding in the active site loop-helix and formation of the disulfide bond, the dimer–dimer interface is perturbed, favoring dissociation of the decamer into dimers and collapse of the loop into the active-site pocket vacated by the peroxidatic Cys [42]. Recently, studies of mutants altering the dimer–dimer interface of AhpC, either stabilizing or disrupting the decameric structure, have fully supported the stabilizing influence of this buttressing effect on efficient catalysis of peroxide reduction within the decamer (Parsonage, Youngblood, Sarma, Wood, Karplus, and Poole, unpublished results). These results agree with other re-

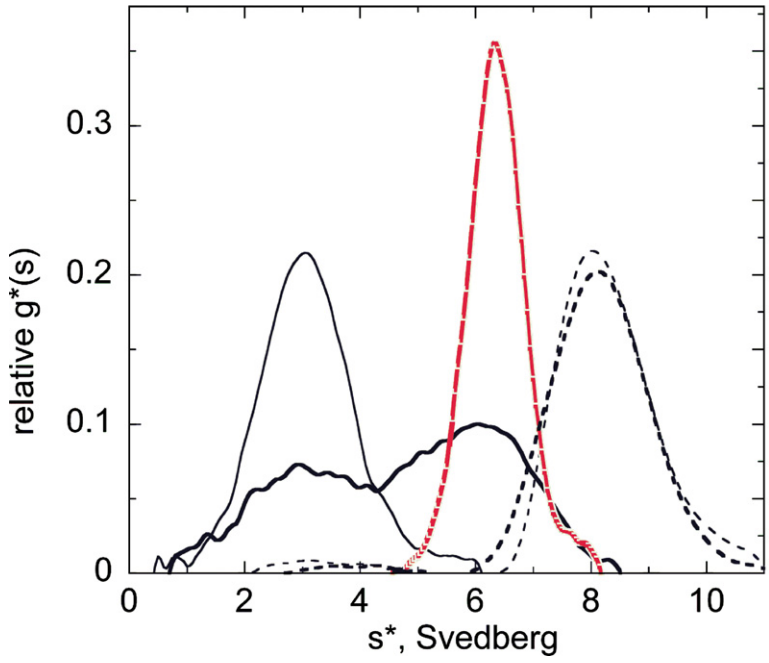

Fig. 9. Sedimentation velocity studies of oxidized and reduced AhpC from *S. typhiumurium*. Oxidized (solid lines) and reduced (dashed lines) AhpC samples at 2.5 μM (thin lines), 12 μM (medium thick lines), and 483 μM (red line) were centrifuged at 42,000 (dashed lines and red line) or 47,000 rpm (thin and medium solid lines). Eight to 12 consecutive data sets at $\omega\Delta^2 t$ values of $0.25–0.55 \times 10^{11}$ s^{-1} were analyzed by DCDT software to give the $g^*(s)$ distributions shown. All plots were normalized by area to ease comparisons. Reprinted with permission from *Biochemistry* [3]. Copyright 2000, American Chemical Society.

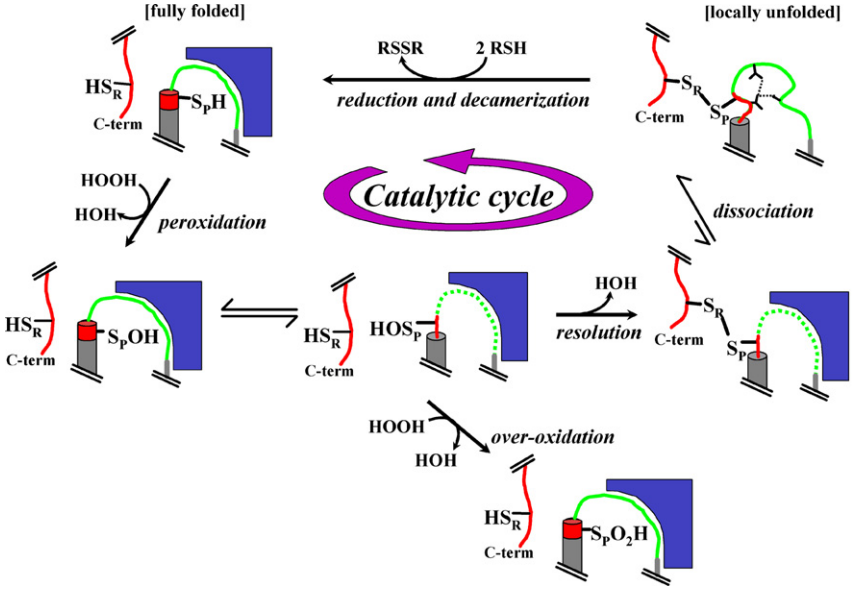

Fig. 10. Redox-sensitive oligomerization of Prxs. This cartoon shows the catalytic cycle of some typical 2-Cys Prxs incorporating information about the alterations in oligomeric state that accompany changes in redox state. The loop-helix region at the active site (residues 40–49), an adjacent region (residues 73–84) from a neighboring homodimer, and the C-terminal arm of a neighboring monomer within the same homodimer are colored green, blue, and red, respectively. The different oxidation states of the peroxidatic cysteine are identified as thiol (S_PH), sulfenic (S_POH) or sulfinic (S_PO_2H) acid forms, or disulfide bonded with the resolving cysteine (S_R). The loop-helix (green plus red) is depicted in folded (red cylinder and solid line) or unfolded (dashed line) conformations, or with the peroxidatic active site restructured (species at upper right). Unidirectional arrows indicate changes in redox state, and bidirectional arrows represent dynamic equilibrium. Reprinted with permission from *Trends in Biochemical Sciences* [42]. Copyright 2002, Elsevier Science Ltd.

ports suggesting that Prx dimers are less active than are the corresponding decameric forms [49]. Regulation of catalytic activity through alterations in oligomeric state may not only apply to other typical 2-Cys Prxs, but may represent an under-recognized phenomenon among other enzyme systems as well [50].

As shown previously for NADH peroxidase and the C165S mutant of AhpC, sulfenic acids at peroxidatic active sites can undergo further oxidation by excess hydroperoxides, forming sulfinic and/or sulfonic acids. Even in 2-Cys Prxs, sulfinic acid formation has been observed both within the crystal structure of the PrxII isolated from human blood [48], and on two-dimensional polyacrylamide gels of eukaryotic Prx proteins separated after direct incubation with peroxides or following treatments eliciting peroxide-mediated cell signaling events [51–53]. The formation of the Cys sulfinic acid in 2-Cys Prxs seems surprising given the presence of the resolving Cys which should react quickly to generate a disulfide bond at the active site. However, because of the large distance between the peroxidatic and resolving Cys residues in the reduced 2-Cys Prxs, and the need for local structural rearrangements in order to permit the generation of a disulfide bond, disulfide bond formation may not be as efficient in some Prxs as it is in others [44,47]. Where the Cys-SOH persists, more opportunity exists for its overoxidation, allowing it to act as a redox sensor or peroxide-sensitive switch in oxidation-sensitive eukaryotic Prxs.

To further investigate the curious phenomenon of Prx overoxidation, we compared structural and functional aspects of a number of bacterial and mammalian enzymes in detail. In fact, bacterial AhpCs exhibit far less sensitivity toward peroxide-mediated inactivation, requiring the presence of 110-fold more hydrogen peroxide to observe inactivation comparable to that detected in Prx I studies [44,53]. This difference highlights the fact that the sensitivity of eukaryotic Prxs toward inactivation by peroxides is an acquired characteristic, rather than an unavoidable consequence of the peroxidatic mechanism. As depicted in Fig. 8A, eukaryotic Prxs contain two structural motifs, including a GGLG motif adjacent to a 3_{10} helix and a YF motif within an extended C-terminal helix, that are absent from the resistant bacterial AhpCs [44]. These two structural features in eukaryotic Prxs cover the catalytic Cys residue making more difficult the conformational changes required for disulfide bond formation (Fig. 8B). In comparison, regions around the peroxidatic Cys and the C-terminus (including the resolving Cys) of *S. typhimurium* AhpC are much more flexible [41], likely facilitating the rearrangements required for efficient disulfide bond formation in these cases (Fig. 8C). Thus, the structural features in eukaryotic Prxs that impart their sensitivity toward inactivation by peroxide are likely to be acquired features allowing these Prxs to take on the dual roles of antioxidant and regulator of peroxide signaling, in contrast to the primary role of Prxs as antioxidants in bacteria. The balance between efficient peroxide removal and inactivation of Prxs by peroxide may have been fine tuned during evolution so that the Prxs can act as a "floodgate," preventing the buildup of toxic hydrogen peroxide levels during normal cellular metabolism, but responding to a rapidly rising burst of signaling levels of hydrogen peroxide through inactivation [44,54]. Consistent with the importance of this balance, the overexpression of Prxs interferes with some known peroxide signaling pathways [49,55].

Regulation of Prx activity by irreversible overoxidation seems wasteful to a cell that has expended energy to synthesize high levels of these antioxidants. Whether this control mechanism comes into play frequently in the life of a cell, or is invoked primarily by cells destined for apoptosis, is not yet known. However, several reports have now identified enzymes which catalyze the regeneration of active Prxs from their sulfinic acid forms [56,57], making even more reasonable our proposal that Prx sensitivity to overoxidation is an important functional attribute allowing these enzymes to regulate hydrogen peroxide-mediated signal transduction in eukaryotes [44,58].

A reversible switch in Prx function induced by disulfide stress: conversion of *E. coli* AhpC into a disulfide reductase by a triplet repeat expansion

In a remarkable discovery by Beckwith and coworkers [59], AhpC in *E. coli* was found to interconvert between its native peroxidase (wild type) form and a new, mutated species (designated AhpC*) without peroxidase activity, but with an apparent new biological function in supplying electrons to the glutathione/glutaredoxin redox system. The notably high rate of spontaneous mutagenesis (0.5×10^{-3}) led to the expansion of a triplet repeat sequence 25 bp upstream of the codon for Cys46, and resulted from engineered deficiencies in both glutathione reductase and TrxR activities in the mutant bacteria (denoted *trxB gor* mutants) which caused increased "disulfide stress." The effect of the resultant amino acid insertion, giving four rather than three phenylalanine residues in a row just prior to the active site loop-helix of AhpC, is to abrogate peroxidase activity, yet support an apparent disulfide reductase activity which can be demonstrated by catalytic reduction of DTNB [59]. This DTNB reductase activity was also observed for the wild type AhpC protein, indicating that the difference between the AhpC- and AhpC*-supported disulfide reductase activity in vivo is probably in their differing substrate specificities, although the identity of the physiological electron acceptor for AhpC* is still unclear. Evidence to date has shown that the ability of an AhpC*-expressing plasmid to complement the dithiothreitol requirement for the growth of *trxB gor* mutants requires expression of AhpF, glutatredoxin 1 and a glutathione synthetic enzyme, but nei-

ther of the two Trx proteins [59]. Perhaps surprisingly, this stress-induced triplet expansion is reversible. On altering the environmental conditions from ''disulfide stress'' to ''oxidative stress'' through additional deletion of the *katG* gene in the *trxB*$^{-}$ *gor*$^{-}$ *ahpC** background, peroxidase activity was restored through reversion of the *ahpC* locus to its wild type sequence. These observations suggest a biological function for this switch between two functional forms of AhpC and a stress-response mechanism for the genetic transformation that is as yet poorly understood.

Cys-dependent Prx systems in other organisms

Studies of Prx systems in several other organisms have pointed to considerable similarities in mechanistic aspects, yet distinct requirements for particular reducing systems, for homologues of AhpC. In those bacterial systems where the AhpC homologues are greater than 55% identical in amino acid sequence with the *E. coli* and *S. typhimurium* proteins, there is invariably an AhpF homologue encoded just downstream of the *ahpC* structural gene. Even the AhpC/AhpF systems of gram positive organisms are extremely similar in mechanistic and structural properties to those from gram negative bacteria; the orthologous proteins from *S. mutans* are readily swapped with the *S. typhimurium* proteins in heterologous systems showing full peroxidase activity [12]. In contrast, more distantly related AhpC homologues including the thiol peroxidase (Tpx) of *E. coli* and the AhpC of *Helicobacter pylori*, which are not encoded by genes proximal to *ahpF* homologues, are also completely unreactive with AhpF as an electron donor, but are able to carry out their peroxidase functions through recycling by TrxR/Trx systems [34,60]. Especially illuminating were the studies of a novel three-protein peroxidase system from *Clostridium pasteurianum*. An operon upstream of the rubredoxin gene in this organism was shown to encode a TrxR homologue (Cp34), a 75-residue glutaredoxin homologue (Cp9) and an AhpC homologue (Cp20) which together catalyze the NADH-dependent reduction of peroxides [61]. Again, AhpF was unable to reduce Cp20 (or Cp9), yet *E. coli* Trx and TrxR could function as the reducing system for Cp20, replacing the Cp34/Cp9 system. Cp34 was an efficient reductant of Cp9, but not Trx, and together these proteins catalyzed not only Cp20 reduction, but also the reduction of more generic disulfide-containing substrates such as insulin. Specialization of reductase systems for other Prx homologues in organisms as diverse as trypanosomes and mycobacteria has also been reported [62,63], suggesting the possibility that such systems could be targeted for inactivation by anti-microbial agents to cripple the antioxidant responses of these invasive organisms.

Summary

The studies described herein have been valuable in elucidating the Cys-based peroxidatic mechanism and structural organization of Prxs which underlie their biological functions in prokaryotic as well as eukaryotic organisms. Through this work, cysteine sulfenic acid was demonstrated to possess both catalytic and regulatory functions at the active sites of eukaryotic Prxs, highlighting the pivotal role these enzymes play in regulating hydrogen peroxide-mediated cell signaling. Coupled enzymological and biophysical studies have elucidated the unusual linkage in these enzymes between oligomeric state, redox state, and peroxidatic activity. As a general rule, Prxs are reactivated during each catalytic cycle by CXXC-containing proteins or modules that themselves receive electrons from reduced pyridine nucleotides (NADH or NADPH) via flavin-mediated electron transfers. The dedicated bacterial Prx reductase, AhpF, achieves the direct transfer of electrons from NADH to AhpC via three redox centers, including FAD and one redox-active disulfide center in the TrxR-like region of the protein, and an additional Trx-like CXXC-containing module at its N-terminus. Electron transfer among all these centers necessarily involves large domain movements during the catalytic cycle. Thus, bacterial AhpC and AhpF proteins have been excellent prototypes in uncovering basic mechanisms involved in the chemistry, structures, and biological functions of peroxide- and disulfide-reducing enzymes.

Acknowledgments

Thanks to present and former members of the Poole laboratory and to our scientific collaborators for their contributions to this work, to Drs. Andy Karplus and Zac Wood for their invaluable experimental and intellectual input and to Zac for preparing many of the figures, and to Dr. Jacque Fetrow for editorial suggestions.

References

[1] M.F. Christman, R.W. Morgan, F.S. Jacobson, B.N. Ames, Cell 41 (1985) 753–762.
[2] L.B. Poole, in: M. Torres, J.M. Fukuto, H.J. Forman (Eds.), Signal Transduction by Reactive Oxygen and Nitrogen Species: Pathways and Chemical Principles, Kluwer Academic Publishers, Dordrecht, The Netherlands, 2003, pp. 80–101.
[3] L.B. Poole, C.M. Reynolds, Z.A. Wood, P.A. Karplus, H.R. Ellis, M. Li Calzi, Eur. J. Biochem. 267 (2000) 6126–6133.
[4] K. Kim, I.-H. Kim, K.Y. Lee, S.G. Rhee, E.R. Stadtman, J. Biol. Chem. 263 (1988) 4704–4711.
[5] H.Z. Chae, K. Robison, L.B. Poole, G. Church, G. Storz, S.G. Rhee, Proc. Natl. Acad. Sci. USA 91 (1994) 7017–7021.
[6] L.B. Poole, A. Claiborne, J. Biol. Chem. 264 (1989) 12330–12338.

[7] L.A. Tartaglia, G. Storz, B.N. Ames, J. Mol. Biol. 210 (1989) 709–719.
[8] L.B. Poole, Biochemistry 35 (1996) 65–75.
[9] H.R. Ellis, L.B. Poole, Biochemistry 36 (1997) 13349–13356.
[10] L.B. Poole, H.R. Ellis, Biochemistry 35 (1996) 56–64.
[11] M. Li Calzi, L.B. Poole, Biochemistry 36 (1997) 13357–13364.
[12] L.B. Poole, M. Higuchi, M. Shimada, M. Li Calzi, Y. Kamio, Free Radic. Biol. Med. 28 (2000) 108–120.
[13] K. Ohnishi, Y. Niimura, K. Yokoyama, M. Hidaka, H. Masaki, T. Uchimura, H. Suzuki, T. Uozumi, M. Kozaki, K. Komagata, T. Nishino, J. Biol. Chem. 269 (1994) 31418–31423.
[14] C. Logan, S.G. Mayhew, J. Biol. Chem. 275 (2000) 30019–30028.
[15] Y. Niimura, V. Massey, J. Biol. Chem. 271 (1996) 30459–30464.
[16] Z.A. Wood, L.B. Poole, P.A. Karplus, Biochemistry 40 (2001) 3900–3911.
[17] L.B. Poole, A. Godzik, A. Nayeem, J.D. Schmitt, Biochemistry 39 (2000) 6602–6615.
[18] C.M. Reynolds, L.B. Poole, Biochemistry 39 (2000) 8859–8869.
[19] B. Ren, G. Tibbelin, D. de Pascale, M. Rossi, S. Bartolucci, R. Ladenstein, Nat. Struct. Biol. 5 (1998) 602–611.
[20] B.W. Lennon, C.H. Williams Jr., M.L. Ludwig, Science 289 (2000) 1190–1194.
[21] T. Jönsson, L.B. Poole, in: R. Perham, N. Scrutton (Eds.), Flavins and Flavoproteins, Agency for Scientific Publications, Berlin, 2002.
[22] C.M. Reynolds, L.B. Poole, Biochemistry 40 (2001) 3912–3919.
[23] L. Chen, Q.W. Xie, C. Nathan, Mol. Cell 1 (1998) 795–805.
[24] H.Z. Chae, S.W. Kang, S.G. Rhee, Methods Enzymol. 300 (1999) 219–226.
[25] L.B. Poole, in: S. Ghisla, P. Kroneck, P. Macheroux, H. Sund (Eds.), Flavins and Flavoproteins, Agency for Scientific Publications, Berlin, 1999, pp. 691–694.
[26] P.-F. Wang, D.M. Veine, S.H. Ahn, C.H. Williams Jr., Biochemistry 35 (1996) 4812–4819.
[27] H.R. Ellis, L.B. Poole, Biochemistry 36 (1997) 15013–15018.
[28] R. Bryk, P. Griffin, C. Nathan, Nature 407 (2000) 211–215.
[29] J.M. Denu, K.G. Tanner, Biochemistry 37 (1998) 5633–5642.
[30] N.A. Kratochwil, A.I. Ivanov, M. Patriarca, J.A. Parkinson, A.M. Gouldsworthy, P.d.S. Murdoch, P.J. Sadler, J. Am. Chem. Soc. 121 (1999) 8193–8203.
[31] S.O. Kim, K. Merchant, R. Nudelman, W.F. Beyer, T. Keng, J. DeAngelo, A. Hausladen, J.S. Stamler, Cell 109 (2002) 383–396.
[32] S.W. Griffiths, J. King, C.L. Cooney, J. Biol. Chem. 277 (2002) 25486–25492.
[33] M. Fuangthong, J.D. Helmann, Proc. Natl. Acad. Sci. USA 99 (2002) 6690–6695.
[34] L.M.S. Baker, L.B. Poole, J. Biol. Chem. 278 (2003) 9203–9211.
[35] J.I. Yeh, A. Claiborne, W.G.J. Hol, Biochemistry 35 (1996) 9951–9957.
[36] T.C. Stadtman, Annu. Rev. Biochem. 49 (1980) 93–110.
[37] Y.M. Torchinsky, in: D. Metzler (Ed.), Sulfur in Proteins, Pergamon, Oxford, England, 1981.
[38] J.R. Kim, H.W. Yoon, K.S. Kwon, S.R. Lee, S.G. Rhee, Anal. Biochem. 283 (2000) 214–221.
[39] E. Mössner, M. Huber-Wunderlich, R. Glockshuber, Protein Sci. 7 (1998) 1233–1244.
[40] L.B. Poole, H.R. Ellis, Methods Enzymol. 348 (2002) 122–136.
[41] Z.A. Wood, L.B. Poole, R.R. Hantgan, P.A. Karplus, Biochemistry 41 (2002) 5493–5504.
[42] Z.A. Wood, E. Schröder, J.R. Harris, L.B. Poole, Trends Biochem. Sci. 28 (2003) 32–40.
[43] J.W. Nelson, T.E. Creighton, Biochemistry 33 (1994) 5974–5983.
[44] Z.A. Wood, L.B. Poole, P.A. Karplus, Science 300 (2003) 650–653.
[45] S.D. Copley, W.R.P. Novak, P.C. Babbitt, Biochemistry 43 (2004) in press.
[46] S. Hirotsu, Y. Abe, K. Okada, N. Nagahara, H. Hori, T. Nishino, T. Hakoshima, Proc. Natl. Acad. Sci. USA 96 (1999) 12333–12338.
[47] M.S. Alphey, C.S. Bond, E. Tetaud, A.H. Fairlamb, W.N. Hunter, J. Mol. Biol. 300 (2000) 903–916.
[48] E. Schröder, J.A. Littlechild, A.A. Lebedev, N. Errington, A.A. Vagin, M.N. Isupov, Structure 8 (2000) 605–615.
[49] B. Hofmann, H.-J. Hecht, L. Flohé, Biol. Chem. 383 (2002) 347–364.
[50] S. Breinig, J. Kervinen, L. Stith, A.S. Wasson, R. Fairman, A. Wlodawer, A. Zdanov, E.K. Jaffe, Nat. Struct. Biol. 10 (2003) 757–763.
[51] A. Mitsumoto, Y. Takanezawa, K. Okawa, A. Iwamatsu, Y. Nakagawa, Free Radic. Biol. Med. 30 (2001) 625–635.
[52] T. Rabilloud, M. Heller, F. Gasnier, S. Luche, C. Rey, R. Aebersold, M. Benahmed, P. Louisot, J. Lunardi, J. Biol. Chem. 277 (2002) 19396–19401.
[53] K.S. Yang, S.W. Kang, H.A. Woo, S.C. Hwang, H.Z. Chae, K. Kim, S.G. Rhee, J. Biol. Chem. 277 (2002) 38029–38036.
[54] L.B. Poole, P.A. Karplus, A. Claiborne, Annu. Rev. Pharmacol. Toxicol. 44 (2004) 325–347.
[55] S.W. Kang, H.Z. Chae, M.S. Seo, K. Kim, I.C. Baines, S.G. Rhee, J. Biol. Chem. 273 (1998) 6297–6302.
[56] B. Biteau, J. Labarre, M.B. Toledano, Nature 425 (2003) 980–984.
[57] A.V. Budanov, A.A. Sablina, E. Feinstein, E.V. Koonin, P.M. Chumakov, Science 304 (2004) 596–600.
[58] G. Georgiou, L. Masip, Science 300 (2003) 592–594.
[59] D. Ritz, J. Lim, C.M. Reynolds, L.B. Poole, J. Beckwith, Science 294 (2001) 158–160.
[60] L.M.S. Baker, A. Raudonikiene, P.H. Hoffman, L.B. Poole, J. Bacteriol. 183 (2001) 1961–1973.
[61] C.M. Reynolds, J. Meyer, L.B. Poole, Biochemistry 41 (2002) 1990–2001.
[62] E. Nogoceke, D.U. Gommel, M. Kiess, H.M. Kalisz, L. Flohé, Biol. Chem. 378 (1997) 827–836.
[63] R. Bryk, C.D. Lima, H. Erdjument-Bromage, P. Tempst, C. Nathan, Science 295 (2002) 1073–1077.
[64] J.P. Declercq, C. Evrard, A. Clippe, D. Vander Stricht, A. Bernard, B. Knoops, J. Mol. Biol. 311 (2001) 751–759.
[65] E. Wagner, S. Luche, L. Penna, M. Chevallet, A.V. Dorsselaer, E. Leize-Wagner, T. Rabilloud, Biochem. J. 366 (2002) 777–785.
[66] M.-K. Cha, C.-H. Yun, I.H. Kim, Biochemistry 39 (2000) 6944–6950.
[67] T. Rabilloud, M. Heller, M.P. Rigobello, A. Bindoli, R. Aebersold, J. Lunardi, Proteomics 1 (2001) 1105–1110.
[68] S.G. Park, M.K. Cha, W. Jeong, I.H. Kim, J. Biol. Chem. 275 (2000) 5723–5732.
[69] K.H. Koo, S. Lee, S.Y. Jeong, E.T. Kim, H.J. Kim, K. Song, H.-Z. Chae, Arch. Biochem. Biophys. 397 (2002) 312–318.
[70] J. König, K. Lotte, R. Plessow, A. Brockhinke, M. Baier, K.J. Dietz, J. Biol. Chem. 278 (2003) 24409–24420.
[71] Y. Niimura, L.B. Poole, V. Massey, J. Biol. Chem. 270 (1995) 25645–25650.